SYNTHESIS OF TIN OXIDE & CADMIUM DOPED TINOXIDE NANO POWDER, PRECIPITATION METHOD

Project Report submitted to

MES ASMABI COLLEGE P.VEMBALLUR

MSc. IN SCIENCE (PHYSICS)

Submitted by

ADIL M ALI

REGISTER NO:

Under the guidance of

DR. EBITHA EQBAL

Department of Physics

MES ASMABI COLLEGE P.VEMBALLUR

Kodungallur-680671

Kerala, India

CERTIFICATE ON PLAGIARISM CHECK

MES ASMABI COLLEGE, KODUNGALLUR

(Affiliated to the University Of Calicut)

1.	Name of the Research Scholar/Student	**ADIL M ALI**		
2.	Title of the Thesis/paper	SYNTHESIS OF TINOXIDE AND CADMIUM DOPED TINOXIDE NANOPOWDER PRECIPITATION METHOD		
3.	Name of the supervisor	Dr. EBITHA EQBAL		
4.	Category	Master's Thesis		
5.	Department/institution	PG Department of Physics		
6.		Introduction / Review of literature	Materials and Methods	Results/ Discussion/summary Conclusion
7.	Similar content (%) identified	-	-	-
	In case Overall similarity (%)	8%		
8.	Revised Check			
9.	Similar content (%) identified		8%	
10	Acceptable Maximum limit			
11	Software used		Plagiarism checker X	
12	Date of Verification		July 13 2024	

Issued by Librarian

Signature of the Researcher Principal / HoD

Signature of the supervisor

Place:

Date: Seal

Plagiarism Checker X - Report

Originality Assessment

Overall Similarity: **8%**

Date: Jul 13, 2024

Statistics: 524 words Plagiarized / 6682 Total words

Remarks: Low similarity detected, check your supervisor if changes are required.

CERTIFICATE

This is to certify that the project work entitled **SYNTHESIS OF TIN OXIDE &CADMIUM DOPED TINOXIDENANO POWDER, PRECIPITATION METHOD** is the work done by Adil m ali at the Department of physics,MES Asmabi college, P.Vemballur, under my guidance in partial fulfillment of the requirements for the fourth-semester course of MSc in science (physics) of MES Asmabi college, P.Vemballur.

Dr.Ebitha Eqbal

Head of the department
Department of Physics

Dr.Ebitha Eqbal

Supervising Teacher
Department of Physics

SYNTHESIS OF TIN OXIDE & CADMIUM DOPED TINOXIDE NANO POWDER, PRECIPITATION METHOD

Submitted by

ADIL M ALI

REGISTER NO:

The project presentation / viva voce held on …….. At M.E.S. Asmabi College, P.Vemballur, is evaluated and approved by

External Examiners:

1.

2.

DECLARATION

I Adil M Ali hereby declare that the Project Report entitled **"SYNTHESIS OF TIN OXIDE &CADMIUM DOPED TINOXIDENANO POWDER, PRECIPITATION METHOD"** submitted towards the partial fulfillment of the requirement for the fourth - semester course of MSc in Science (Physics), MES Asmabi college, P.Vemballur is an original work written and composed entirely by me under the guidance of Dr.Ebithha Iqbal, Department of Physics, MES Asmabi college, P.Vemballur-680668.

I also declare that the information embodied in this report is authentic to the best of my knowledge and the references I have been duly cited and the external sources used in this project report have been properly referenced.

Adil m ali
MSc physics
MES Asmabi college, P.Vemballur

ACKNOWLEDGEMENT

This project titled “SYNTHESIS OF TIN OXIDE &CADMIUM DOPED TINOXIDENANO POWDER, PRECIPITATION METHOD” is carried out by the Department of Physics, MES Asmabi college, under the guidance of Dr.Ebitha Iqbal, Professor, Department of Physics, MES Asmabi college, P.Vemballur. I am extremely thankful to my project guide, Dr.Ebitha Iqbal,whose immense support and valuable ideas make this project successful. I am thankful to Dr.Sheena PA, Head of Department, Department of Physics, MES Asmabi college, for providing the infrasrequirements. I sincerely thank my parents and everyone who has helped and encouraged me to make this project a reality.

ABSTRACT

Nanotechnology has emerged as a highly promising area of research with significant applications across all fields of science. Tin oxide has garnered substantial attention due to its remarkable properties, which are further enhanced when synthesized at the nanometer scale. Various physical and chemical methods are currently employed to produce tin oxide nanoparticles. Among these, chemical precipitation serves as a promising method to develop nanocatalysts. By simply mixing precursor solutions and inducing precipitation through chemical reactions, this method proves accessible to researchers and industries with limited resources. The precipitation method for nanoparticle synthesis offers a straightforward and economical approach for producing nanoparticles.

For the comparison study, we prepared two types of samples: pure tin oxide and cadmium-doped tin oxide nanopowders. Tin Oxide (SnO_2) and cadmium-doped tin oxide nanoparticles powder have been synthesized by the chemical precipitation method. The samples were characterized by X-ray diffraction (XRD), UV-Visible absorption spectroscopy, and scanning electron microscopy (SEM).

The Powder X-ray Diffraction (XRD) method has been extensively employed to analyze the crystal structure, lattice parameters, stresses, and crystallite size of nanoparticles. The XRD pattern revealed peaks indicating that both the tin oxide and the cadmium-doped tin oxide exhibit tetragonal structures. The average grain size was reduced from 12.6 nm to 10.54 nm by doping.

UV-Visible absorption spectroscopy, based on the measurement of light absorption due to electronic transitions in a sample, is widely used to quantitatively characterize nanomaterials. The analysis revealed a band gap energy of 3.4 eV for pure SnO_2 nanopowder and 3.3 eV for Cd-doped SnO_2 nanopowder.

Scanning Electron Microscopy (SEM) is a crucial analytical technique used in nanoparticle synthesis to characterize the morphology, size, and surface structure of nanoparticles. SEM provides high-resolution images by scanning a focused beam of electrons across the sample's surface, revealing granular structures of both compounds.

To analyze the photocatalytic property, the nanopowder solution was mixed with methyl orange dye, and the absorption spectra were measured after 24 and 48 hours. The results indicated a degradation in absorbance percentage over time, demonstrating the photocatalytic activity of the nanoparticles.

CONFERENCE ATTENDED

1.Presented a poster in the National Conference on Light Matter Interaction and Spectroscopy (NCLMIS 2024) held on 25th March 2024.

DEPARTMENT OF PHYSICS
MES ASMABI COLLEGE

NCLMIS 2024

CERTIFICATE

This is to certify that

Adil. M. Ali

~~participated~~/~~presented a paper~~/presented a poster in the National Conference on Light Matter Interaction and Spectroscopy (NCLMIS 2024) held on March 25, 2024. Your active involvement contributed to the success of the event, enriching discussions and fostering academic exchange.

Prof. A. Biju
Principal

Dr.Sheena P.A.
H.O.D

Dr. Ebitha Eqbal
Coordinator

LIST OF FIGURES

LIST OF TABLES

CONTENTS

CHAPTER 1

Introduction

1.1 Nanotechnology

Nanotechnology is the construction and use of functional structures designed from atomic or molecular scale with at least one characteristic dimension measured in nanometers. Their size allows them to exhibit novel and significantly improved physical, chemical, and biological properties, phenomena, and processes because of their size. Thus, nanotechnology can be define as research and development that involves measuring and manipulating matter at the atomic, molecular, and supramolecular levels at scales measured in approximately 1–100 nm in at least one dimension.

Nanoparticle with a size of 1 nm is smaller by 10^4 times than an object of 10 μm in size. In addition, this single micrometer-sized particle is equivalent to 10^{12} nanoparticles by mass. This simple comparison makes it clear that nanoparticles are really very small and also expose a large fraction of atoms on their surfaces.

In the last few decades, the technologies for the fabrication of integrated circuits have made the smallest structure (i.e., <100 nm) elements of microelectronic chip devices by mass production. Thus, due to multifunctional miniaturization, cell phones are becoming tinier, laptops are getting lighter, and a thin strand of optical fiber is replacing thick bundles of copper telephone wire.

1.2 Nanopowder

Nano powder typically refers to nanoscale powder or nanoparticles. Nanopowders can be composed of various materials such as metals, oxides, ceramics, or polymers. They find applications in a wide range of fields, including electronics, medicine, catalysis, energy storage, and coatings, among others. The specific properties of nanomaterials make them attractive for different purposes. For example, they may have enhanced electrical or thermal conductivity, improved mechanical strength, or unique optical properties. However, the use of nanomaterials also raises concerns about potential health and environmental impacts, and researchers are actively studying these aspects to ensure the safe use of nanotechnology.

1.3 Applications of nanoparticles

Nanoparticles, those ultrafine units with dimensions measured in nanometres (nm), have unique material characteristics due to their submicroscopic size. They exist naturally and are also created

through human activities. These tiny particles find practical applications across various fields, including medicine, engineering, catalysis, and environmental remediation .

Let’s delve into some of the fascinating applications of nanoparticles:

1. Healthcare Industry:
    - Drug Delivery: Nanoparticles play a crucial role in drug delivery. For instance, they can help transport chemotherapeutic medications directly to cancerous tumors or damaged areas of arteries for cardiovascular disease treatment.
    - Bacterial Sensors: Efforts are underway to develop nanoparticles for creating bacterial sensors by attaching antibodies to nanotubes.

2. Aerospace Applications:
    - Carbon Nanotubes: These remarkable materials are used in aerospace applications, including morphing aircraft wings. When an electric voltage is applied, a composite made of nanotubes bends, allowing for adaptive wing shapes.

3. Environmental Preservation:
    - Nanowires: Nanomaterials like zinc oxide nanowires are employed for environmental preservation. They contribute to flexible solar cells and the remediation of contaminated water.

4. Cosmetics Sector:
    - UV Protection: Mineral nanoparticles, such as titanium oxide, are used in sunscreen. They provide effective UV protection while minimizing the unsightly whitening effect often seen with traditional chemical sunscreens.

5. Sports Equipment:
    - Carbon Nanotube Baseball Bats: Carbon nanotubes are incorporated into baseball bats, making them lighter and enhancing performance.
    - Antimicrobial Nanotechnology: Nanoparticles are also used in sports goods like towels and mats to prevent bacterial illnesses.

In summary, nanoparticles are revolutionizing various industries, from healthcare to cosmetics, by leveraging their unique properties and precise manufacturing capabilities

1.4 Synthesis Techniques

There are many methods to classify synthesis techniques of nanomaterials, broadly categorized into top-down and bottom-up approaches. The top-down approach includes techniques such as mechanical alloying, nanolithography, electron-beam lithography, X-ray lithography, soft lithography, and severe plastic deformation. On the other hand, the bottom-up approach encompasses methods like physical vapor deposition, chemical vapor deposition, colloidal route, green chemistry route, and sol-gel method, which involve the buildup of atoms or molecules layer by layer. Generally, nanoparticles, nanoplatelets, and nanotubes are energetically unfavorable on their own. Thus, their properties are often exploited by embedding them in polymer, metal, or ceramic matrices to create thermodynamically stable nanocomposites.

1.5 Tin Oxide Nanoparticles

1.5.1 Structure and Properties

Tin oxide nanoparticles can have various crystal structures, but the most common is cassiterite (SnO_2), which is a tetragonal crystal structure composed of tin atoms bonded to oxygen atoms.

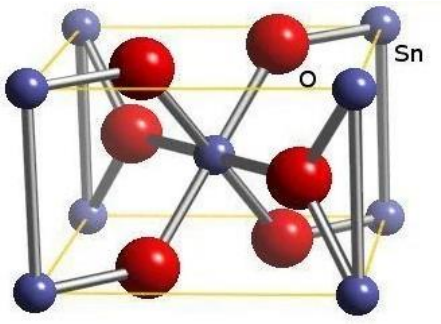

Fig 1.1. Structure of SnO_2

In cassiterite, each tin atom is surrounded by six oxygen atoms in an octahedral arrangement, forming a distorted rutile structure. The crystal lattice is held together by strong covalent bonds between tin and oxygen atoms.

Tin oxide nanoparticles exhibit several interesting properties:

1.Electrical conductivity: Tin oxide nanoparticles can exhibit either n-type or p-type conductivity depending on their preparation methods and doping. N-type conductivity arises from excess oxygen vacancies, while p-type conductivity results from doping with elements like fluorine or antimony.

2. Optical properties: Tin oxide nanoparticles are transparent in the visible range and have a wide bandgap, making them suitable for applications in transparent conductive coatings for displays, solar cells, and optoelectronic devices.

3. Gas sensing: Tin oxide nanoparticles are highly sensitive to various gases, including carbon monoxide, nitrogen dioxide, and volatile organic compounds. Changes in conductivity upon exposure to these gases make tin oxide nanoparticles useful for gas sensing applications, such as environmental monitoring and industrial safety.

4. Catalytic activity: Tin oxide nanoparticles possess catalytic activity, particularly in oxidation reactions. They are employed as catalysts in various industrial processes, including gas-phase reactions and environmental remediation.

1.5.2 Synthesis method

Precipitation method :

Nanoparticles of tin dioxide have been synthesized using various chemical routes, including precipitation, hydrothermal, sol–gel, hydrolytic, carbothermal reduction, and polymeric precursor methods. Despite efforts to prevent agglomeration, it is almost inevitable due to the small diameter of the oxide particles and the presence of compounds involved in these procedures, particularly solvents. Among the various strategies for developing nanoparticles, chemical precipitation stands out as a promising method for producing nanocatalysts, as it facilitates the complete precipitation of metal ions. Additionally, this method is commonly used to prepare

nanoparticles with higher surface areas.

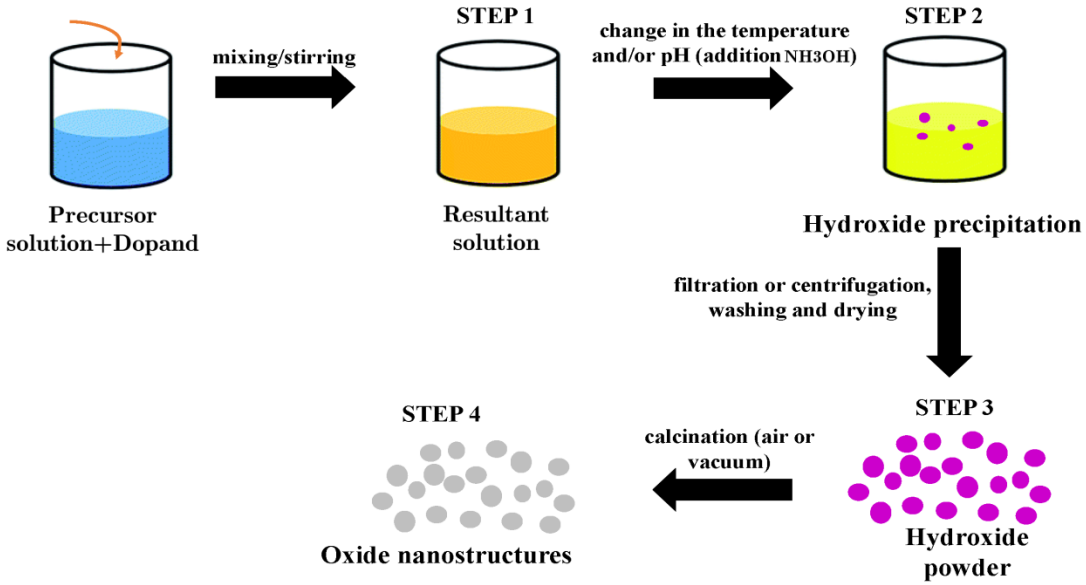

Fig 1.2. Schematic representation of precipitation method

A chemical precipitation process consists of three main steps: chemical reaction, nucleation, and crystal growth. Generally, chemical precipitation is not a controlled process in terms of reaction kinetics and the solid phase nucleation and growth processes. As a result, the solids obtained through chemical precipitation typically exhibit a wide particle size distribution, uncontrolled particle morphology, and significant agglomeration. To obtain nanoparticles with a narrow size distribution, the following requirements must be met: (i) a high degree of supersaturation, (ii) a uniform spatial concentration distribution within the reactor, and (iii) a uniform growth time for all particles or crystals.

The precipitation method for nanoparticle synthesis offers a straightforward and economical approach for producing nanoparticles. By simply mixing precursor solutions and inducing precipitation through chemical reactions, this method proves accessible to researchers and industries with limited resources. Moreover, its scalability allows for the synthesis of nanoparticles in bulk quantities, catering to the demands of industrial applications. One of its significant advantages lies in the control it affords over particle size and morphology. Through adjustment of parameters such as temperature, pH, and reactant concentrations, researchers can finely tune the characteristics of the synthesized nanoparticles to meet specific requirements. Additionally, the precipitation method typically yields a high percentage of desired nanoparticles, thereby reducing production costs and minimizing waste. Its versatility extends to a wide range of materials, including metal oxides, metal sulfides, and metal hydroxides, enabling the creation of

nanoparticles tailored for diverse applications. Furthermore, this method is environmentally friendly, often employing benign reactants and conditions. With compatibility for continuous processing, it facilitates ongoing production while reducing agglomeration, resulting in well-dispersed nanoparticles suitable for various applications, from catalysis to biomedicine. Overall, the precipitation method stands as a valuable technique in nanoparticle synthesis, combining simplicity, scalability, tunability, and environmental friendliness to meet the demands of modern research and industry.

1.5.3 Applications

SnO_2 is a promising candidate for various applications due to its wide energy gap (3.6 to 3.8 eV), strong thermal stability (up to 500 °C), high degree of transparency in the visible spectrum, and robust chemical and physical interactions with adsorbed species. These properties make SnO_2 suitable for use in lithium-ion batteries, sensors, catalysis, energy storage, glass coatings, medicine, and environmental remediation. Its high specific surface area, high chemical stability, low electrical resistance, and low density enhance its performance as a sensor, improving response time and sensitivity. Over recent years, SnO_2 has been extensively researched for applications in solar cells and gas sensors, particularly for detecting combustible gases such as CO, NO, NO_2, H_2S, and C_2H_5OH. Due to the unique physicochemical properties and potential applications of nanoparticles (NPs), the scientific community continues to develop various methods for producing these nanoparticles.

CHAPTER 2

EXPERIMENTAL METHOD AND CHARACTERISATION TECHNIQUES

2.1 Experimental

2.1.1. Powder Prepration

To begin the powder preparation process, the initial step involves cleaning the beakers, spatula, and glass rod meticulously with a combination of distilled water and acetone. Before utilizing the weighing machine, it's imperative to switch it on and allow it to stabilize for a duration ranging from 5 to 15 minutes. For weighing purposes, the spatula is cleaned with acetone, and then it is used to retrieve the salt from its respective container. Similarly, the weighing machine is also cleaned with acetone, ensuring it is properly calibrated to zero, and a piece of butter paper is placed on it. Subsequently, the salt is added onto the butter paper and weighed accordingly.

For the synthesis of SnO_2nano powder, 1.12g (0.125 molar) of stannous chloride dihydrate (SnCl2.2H2O) is dissolved in 20 ml of distilled water. Additionally, 0.1g of CTAB is dissolved in 20 ml of distilled water and added to the stannous chloride solution. The resultant solution is then subjected to magnetic stirring for 15 minutes. Gradually, sodium hydroxide solution is introduced dropwise into the tin chloride solution while ensuring constant stirring to act as a precipitating agent and maintain the pH of the solution. Upon the addition of ammonium hydroxide solution, a precipitate forms within the solution, reaching a pH value of 10. Subsequently, stirring is ceased, and the precipitate is dried in an oven at 300°C for 4 hours. Following the drying process, the material is subjected to calcination in a muffle furnace. The resulting solid matter is finely ground into powder form and stored in a bottle for further use, undergoing subsequent characterization techniques.

For the synthesis of Cd-doped SnO_2nano powder, 4.28g of stannous chloride dihydrate is dissolved in 20ml of distilled water, and 0.911g of CTAB is added to the solution. Separately, 0.2283g of Cadmium Chloride is dissolved in 20 ml of distilled water in another beaker. Both solutions are subjected to magnetic stirring for 5 minutes individually before being combined and stirred for an additional 15 minutes. The pH of the solution is maintained at 8 by the gradual addition of ammonium hydroxide while stirring continuously. Similar to the process for SnO_2 nano powder synthesis, the solution is allowed to settle, stirring is halted, and the precipitate is dried in an oven at 300°C for 4 hours followed by calcination in a muffle furnace. The resulting solid matter is then ground into powder and stored for further analysis using various characterization techniques.


Fig 2.1 (a) Weighing balance *(b) Hot air oven* *(c) Muffle furnace*

2.1.2 Analysis of Photo catalytic action of pure and Cadmium doped TinOxide nanopowder

To observe the photo catalytic action of $SnO_2$and Cd doped SnO_2nanopowders need some experimental procedures. The arrangements are set for the experimental procedure. We require 4 clean beakers, prepared cadmium-doped and pure tin oxide nanopowders, two spatulas, distilled water, and a small amount of methyl orange. Label two beakers as 'Pure SnO_2' and the other two as 'Cd-doped SnO_2'. Add 30 ml of distilled water to all 4 beakers.

Using the clean spatulas, weigh and add 0.01g of pure tin oxide and Cd-doped tin oxide into the appropriate beakers. Within each solution, add one drop of methyl orange to all 4 beakers, mix well, and cover the top of each beaker with foil paper. Place two beakers under light (labeled as Cd-doped and pure SnO_2) and the other two in dark places for 42 hours.

After 24 hours, extract a small amount of solution from each of the four beakers into four clean glass bottles. Observe any color changes and use this for UV-visible spectroscopy analysis. Repeat this process after 42 hours, again taking a small amount of solution from each beaker for UV-visible spectroscopy analysis.

2.2 Characterisation techniques

The characterization of particle size, size distribution, morphology, and composition can be achieved through two fundamental methods: the direct method and the indirect method. The direct method involves inspecting particles and making actual measurements of their dimensions, while the indirect method relies on understanding the relationship between particle behavior and its size. In this chapter, we will delve into the basic principles and applications of various characterization techniques, including powder X-ray diffraction (XRD), UV-visible (UV-Vis) spectroscopy, scanning electron microscopy (SEM)

2.2.1 X–Ray Diffraction

Fig 2.2 Aeris XRD Instrument

The Powder X-ray Diffraction (XRD) method has been extensively employed to analyze the crystal structure, lattice parameters, stresses, and crystallite size of nanoparticles. This technique utilizes energetic X-rays capable of penetrating deep into materials, offering insights into bulk structure. In XRD, a monochromatic X-ray beam with a wavelength typically ranging from 0.7 to

2 Å is directed onto a specimen. The X-rays undergo diffraction by the crystalline phases in the specimen, following Bragg's law:

$$n\lambda = 2d\sin\theta$$

Here, n represents the order of diffraction, d denotes the spacing between atomic planes in the crystalline phase, and λ stands for the X-ray wavelength. The intensity of the diffracted X-rays is recorded as a function of the diffraction angle 2θ and the specimen's orientation. This diffraction pattern aids in identifying the specimen's crystalline phases and measuring its crystallite size.

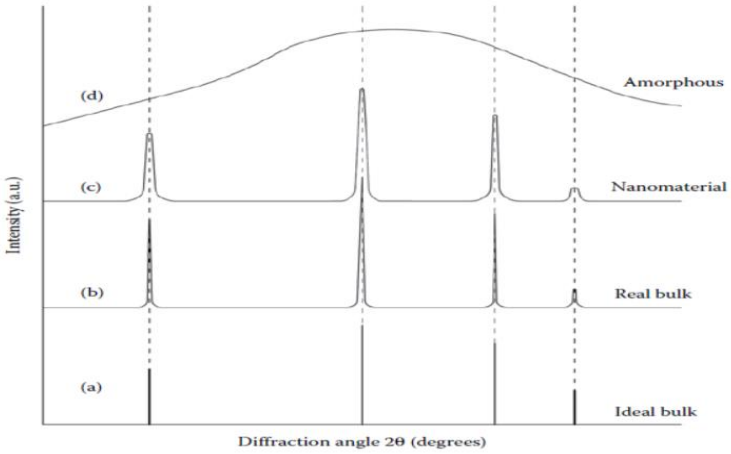

Fig 2.3 Typical XRD patterns of ideal bulk, real polycrystalline bulk, polycrystalline nanomaterials and amorphous metallic materials.

The XRD pattern acts akin to a fingerprint, facilitating the differentiation of mixtures comprising various crystalline phases. This is achieved by comparing their XRD patterns with reference data from electronic databases like the Inorganic Crystal Structure Database (ICSD).

The Debye–Scherrer equation is commonly employed to calculate the crystallite size and strain of the sample. In the absence of inhomogeneous strain, the average crystallite size t is determined from the full width at half maximum (FWHM) of a diffraction peak broadening using the Debye–Scherrer equation:

$$t = \frac{k\lambda}{\cos\theta\ \beta_c}$$

Here, t represents the crystallite size, and βc denotes the corrected FWHM. The Scherrer's constant k varies for diffractions with different crystallographic Miller indices (hkl) of a cubic crystal lattice; however, it is generally assumed to be 0.9 for simplicity in cubic materials.

2.2.2 UV–Vis Spectroscopy

Fig 2.4 UV-Visible Spectrometer

It is based on the measurement of light absorption due to electronic transitions in a sample and is widely used to quantitatively characterize the nanomaterials.The electronic absorption spectroscopy is often called UV–vis spectroscopy because of the wavelength of light required for electronic transitions is typically in the ultraviolet and visible region.

UV–visible spectroscopy is one of the simplest and most useful optical techniques for studying optical properties of nanomaterials.A beam of monochromatic light (300–800 nm) is split into two beams, one of them is passed through the sample and the other passes a reference. The sample should be of low concentration and free from any kinds of foreign particles. After transmission through the sample and reference, two beams are directed back to the light detectors, photomultiplier tube (PMT) or charge-coupled device (CCD), where they are compared. If the

sample absorbs light at some wavelength, the transmitted light will be reduced. Then, the intensity of the transmitted light is plotted as a function of the wavelength of light.

From a given energy bandgap of a semiconductor, the wavelength of the color transmitted is calculated by using the following equation:

$$\Delta E = \frac{hc}{\lambda}$$

where *c* is the velocity of light. The position of absorption maxima for a molecule depends on the difference in the energy of the ground-state level to that of excited state. Larger is the difference between the energy of ground state and excited state, higher is the frequency of absorption and thus smaller will be the wavelength.

2.2.3 Scanning Electron Microscopy

Fig 2.5 Carl Zeiss Sigma FESEM

Electron microscopy became one of the most important techniques to characterize the material's morphology on the nanometer to atomic scale. There are two main types of electron microscopes: SEM and TEM.

When the electron beam (energy 5–30 keV) impinges on the specimen, many types of signals are generated including SEs and BSEs. Most of the electrons are scattered at large angles (from 0° to 180°) when they interact with the positively charged nucleus. These elastically scattered electrons are usually called Back Scattered Electrons (BSEs). Some electrons are scattered inelastically due to the loss in kinetic energy upon their interaction with orbital shell electrons, these electrons are called Secondary Electrons (SEs). The SEs as well as BSEs are widely used for SEM topographical imaging. The lateral spatial resolution of a SEM image is affected by the size of the volume from where the signal electrons escape.

A typical SEM has an image resolution of 5–10 nm, but a modern state-of-the-art SEM like field emission SEM is capable of providing an image resolution of 1 nm. The SEM has advantages of providing a large depth of focus due to the short wavelength of the primary electron beam used, a larger imaging field of view, and 3-D image or topography of the sample than the TEM. SEM is often combined with energy-dispersive x-ray (EDX) spectroscopy detector to get the elemental composition of the nanomaterials.

A specimen for SEM analysis can be in any form (powder or pieces) and size, which is easily fitted on specimen holder.

CHAPTER 3

RESULT AND DISCUSSION

3.1 PURE TIN-OXIDE NANO POWDER

3.1.1 XRD Analysis

The structural properties of the samples were investigated through X-ray diffraction (XRD) pattern analysis. The growth of the nano powder is influenced by various factors such as the precursor composition, reaction conditions and reaction time. XRD is commonly employed for studying the crystallography of materials. In our analysis, we generated a graph with 2θ on the X-axis and Intensity on the Y-axis using Origin software. The obtained data was compared with values from the JCPDS data.

For tin oxide, the X-ray diffraction pattern revealed peaks at 2θ angles of 26.588,33.849,37.950,51.771 and 54.764 degrees, corresponding to the Miller indices (1 1 0), (1 0 1), (2 0 0), (2 1 1), and (2 2 0), respectively. This indicates that the tin oxide exhibit tetragonal structures.

To determine the average grain size of the samples, we utilized the Debye-Scherrer formula:

$$\boldsymbol{D = \frac{0.9\,\lambda}{\beta\,cos\theta}}$$

Where:

- D represents the average grain size.

- λ is the wavelength of X-ray radiation.

- β is the full width at half maximum (FWHM) of the diffraction peak.

- θ is the glancing angle.

This formula allows us to evaluate the grain size based on the XRD data obtained.

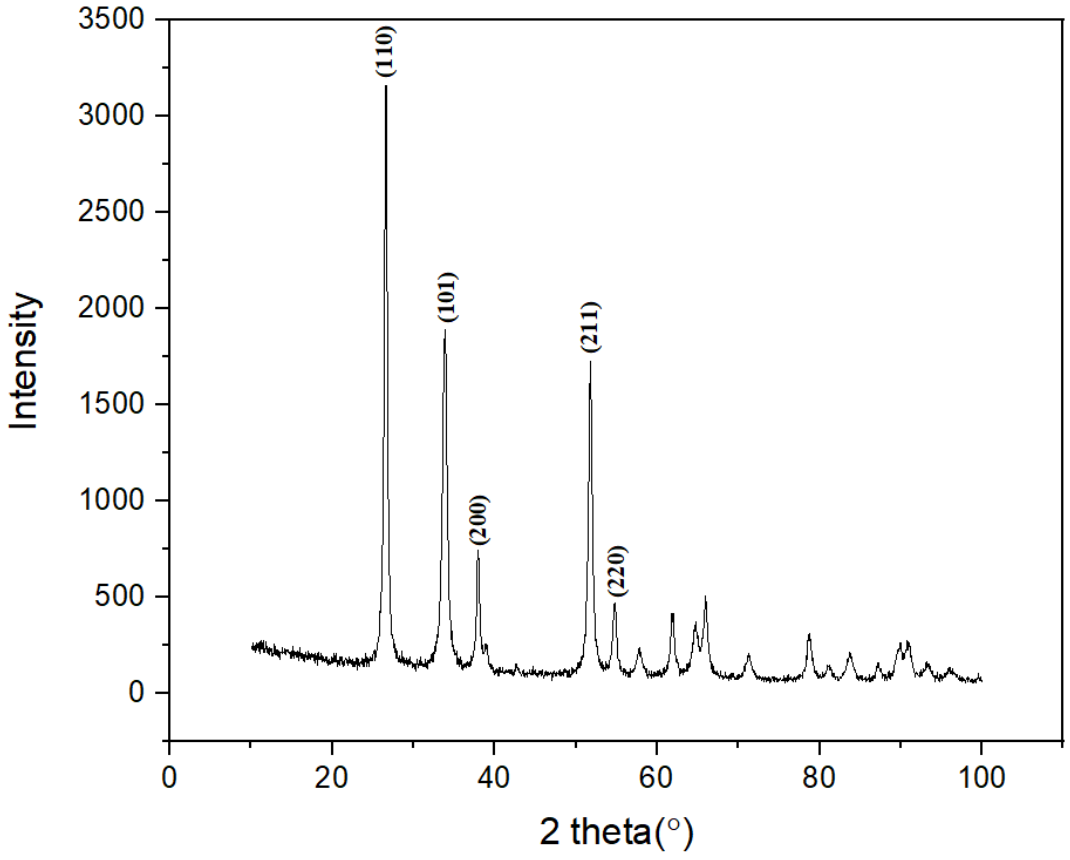

Fig 3.1 XRD Analysis graph of pure TinOxide Nanopowder

3.1.1 (a) Crystalline size

To calculate the crystalline size and average crystalline size from XRD data, we first need to identify the peaks corresponding to the crystal planes of interest in the X-ray diffraction (XRD) pattern. These peaks provide information about the structural characteristics of the material. Once the peaks are identified, we measure the full width at half maximum (FWHM) of each peak, representing the angular width at half of its maximum intensity. We also determine the peak position (θ) in radians.

With these values in hand, we can then use the Scherrer equation, given by:

$$\boldsymbol{D = \frac{0.9\,\lambda}{\beta\,cos\theta}}$$

where D is the crystalline size (in nanometers), λ is the wavelength of the X-ray source (usually 0.15418 nm), β is the FWHM in radians, θ is the peak position in radians, and 0.9 is a constant factor commonly used.

Substituting the measured values of β and θ, along with the known values of λ and 0.9, into the Scherrer equation allows us to calculate the crystalline size for each peak. If multiple peaks are analyzed, the average crystalline size can be determined by taking the mean of the individual crystalline sizes obtained from each peak.

This approach provides valuable insights into the structural properties of materials, aiding in the characterization and understanding of their crystalline nature.

XRD Peak position 2θ (deg)	FWMH β (deg)	Bragg's Peaks h k l	Crystalline size D(nm)	Average D(nm)
26.58845	0.52442	1 1 0	14.74276037	12.59982975
33.84902	0.73292	1 0 1	10.36977436	
51.77104	0.62373	2 1 1	11.45884232	
54.76475	0.51014	2 2 0	13.82794194	

Table 3.1Crystalline size of SnO_2 calculated using Debye Scherrer's Equation

The dislocation density defined as the length of dislocation lines per unit volume is calculated from the crystalline size D using the equation

$$\text{dislocation density } (\delta) = \frac{1}{D^2}$$

$$\delta = \frac{1}{12.5998^2}$$

$$\delta = 0.0063$$

3.1.1(b) Texture Coefficent

Texture coefficient analysis provides insights into the preferred orientation of crystalline domains within nanoparticles, which is investigated by calculating the texture coefficient TC(hkl) for the plane from the following equation:

$$TC(hkl) = \frac{I(hkl)}{\frac{1}{N} \Sigma I(hkl)}$$

where TC(hkl) is the texture coefficient of the hkl plane, I(hkl) is the intensity of each plane and N is the number of reflections. A high TC value indicates a strong orientation preference of crystalline domains along a specific crystallographic plane in nanoparticles, which can have significant implications for their properties and applications.

hkl value	TC(hkl)
1 1 0	**1.53**
1 0 1	**1.139**
2 0 0	**0.98**
2 1 1	**0.33**

Table 3.2 texture coefficent of each hkl plane for SnO_2 NPs

3.1.1(c) d-Spacing or Interplanar Spacing

To determine the interplanar spacing (d spacing) from XRD data using Bragg's equation, we employ the formula:

$$d = \frac{n\lambda}{2d \sin\theta} \qquad (1)$$

Where:

- $\lambda = 1.5418$ Å (wavelength of incident X-ray)

- θ represents the peak position (in radians)

- n = 1 (order of diffraction)

- d is the interplanar spacing or d spacing (in Å)

Initially, we need to identify the peak position from the XRD data. Then, by substituting this value into equation (1), we can calculate the interplanar spacing.

2 theta (deg)	theta (deg)	d-spacing (Å)
26.58839	13.2942	3.349842101
33.84889	16.92445	2.646075279
37.95008	18.97504	2.369015091
51.771	25.8855	1.764419747
54.76341	27.38171	1.674870063
57.80906	28.90453	1.593663912
61.8902	30.9451	1.498007124
64.77052	32.38526	1.438174468
65.94984	32.97492	1.415285335
71.27829	35.63915	1.321998659
78.73052	39.36526	1.214482598
83.81602	41.90801	1.153253161
89.85654	44.92827	1.09073508
90.86845	45.43423	1.081205749

Table 3.3 d spacing of SnO_2 calculated using bragg's equation.

3.1.1 (d) Grain size from WH Plot

The diffraction line broadening caused by the strain and reduced grain size was analyzed using the Williamson-Hall (W-H) method.

The relation used for the calculation of lattice strain and crystalline size is

$$\beta \cos\theta = 0.9\,\lambda/D + 2\xi \sin\theta \qquad (2)$$

Where ξ represents the lattice strain, β is the full width at half maximum of the diffraction peak, and θ is the glancing angle and D is the average grain size calculated using Scherrer's formula.

Eqution (2) can be rewrite as

$$\beta \cos\theta = \xi\,(2\sin\theta) + 0.9\,\lambda/D \qquad (3)$$

Equation (3) represents a straight line,in which ξ is the gradient (slope) of the line and $0.9\,\lambda/D$ is the y-intercept.

Consider the standard equation of a straight line,

$$y = mx + c \qquad (4)$$

where 'm'is the slope of the line and 'c' is the y-intercept.
Comparing equation (3) with equation (4) we have,

y = β cosθ
m=ξ
x=2 sinθ
c=$0.9\,\lambda/D$

The value of 'm' represents gradient (slope) of the line so it will be the value of strain "ξ".and finally we calculate the the crystallite size from the y-intercept " $0.9\,\lambda/D$ "

The plot of 2sinθ on x-axis and βcosθ on y-axis is shown below.

2Theta (Deg)	Theta (Rad)	FWMH (Deg)	FWMH (Rad)	β COSθ	2sinθ
26.58845	0.232027998	0.52442	0.009152856	0.008908	0.459903
33.84902	0.295388424	0.73292	0.012791867	0.012238	0.582223
51.77104	0.451787553	0.62373	0.010886142	0.009794	0.873149
54.76475	0.477912601	0.51014	0.008903623	0.007906	0.919853

Table 3.4 values of βcosθ and 2sinθ for SnO_2 NPs .

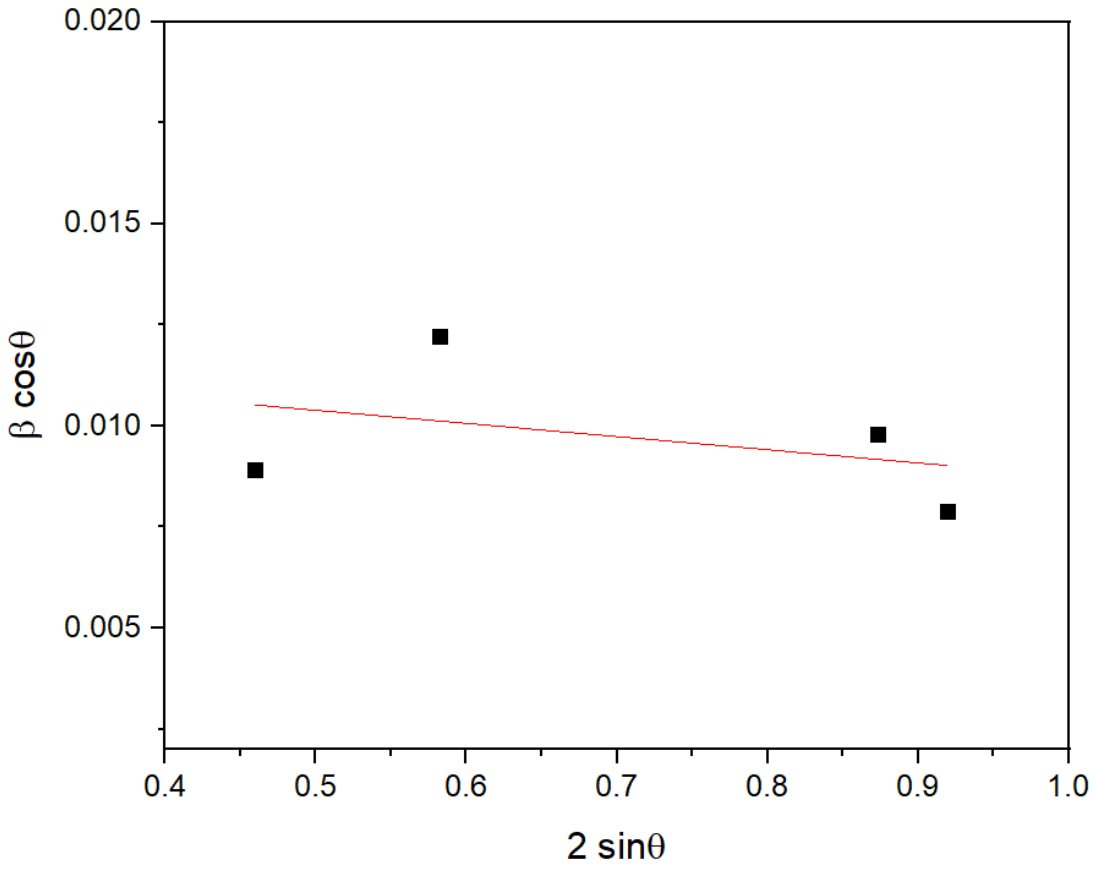

Fig 3.2 To calculate crystalline size and strain from XRD data using Williamson-Hall (W-H) plot method.

Slope of the plot is the strain.So the value of strain (ξ) = -0.00326
The value of y-intercept "c" = 0.01202

$$\text{y-intercept } \mathbf{c}=0.9\ \lambda/D$$

Or

$$D=0.9\ \lambda/c$$

Where the shape factor and λ = 0.15406 nm is the wavelength of the X-ray source,putting all these values we get,

$$D = \frac{0.9 \times 0.15406}{0.0129}$$

$$D = \frac{0.138654}{0.0129}$$

$$D = 10.748 \text{ nm}$$

COMPOUND	Grain size (D) from Scherrer's Formula (nm)	Grain size (D) from W-H plot (nm)
PURE TIN OXIDE NANOPOWDER	**12.6**	**10.748**

Table 3.5 Grain size comparisson data of SnO_2 from Debye Scherrer's Equation and W-H plot

3.1.2 Scanning Electron Microscope (SEM)

The SEM images taken at the magnification of 10μm,5μm,1μm the resultant image depict the agglomerated SnO_2 nanoparticles through Precipitation method. It is not possible to predict the exact size of the individual particle, wich can be done through TEM analysis. From the

micrograph, it can be guessed that the particles are irregular in shape, but for the size of the particles, particle analyzer was done further.

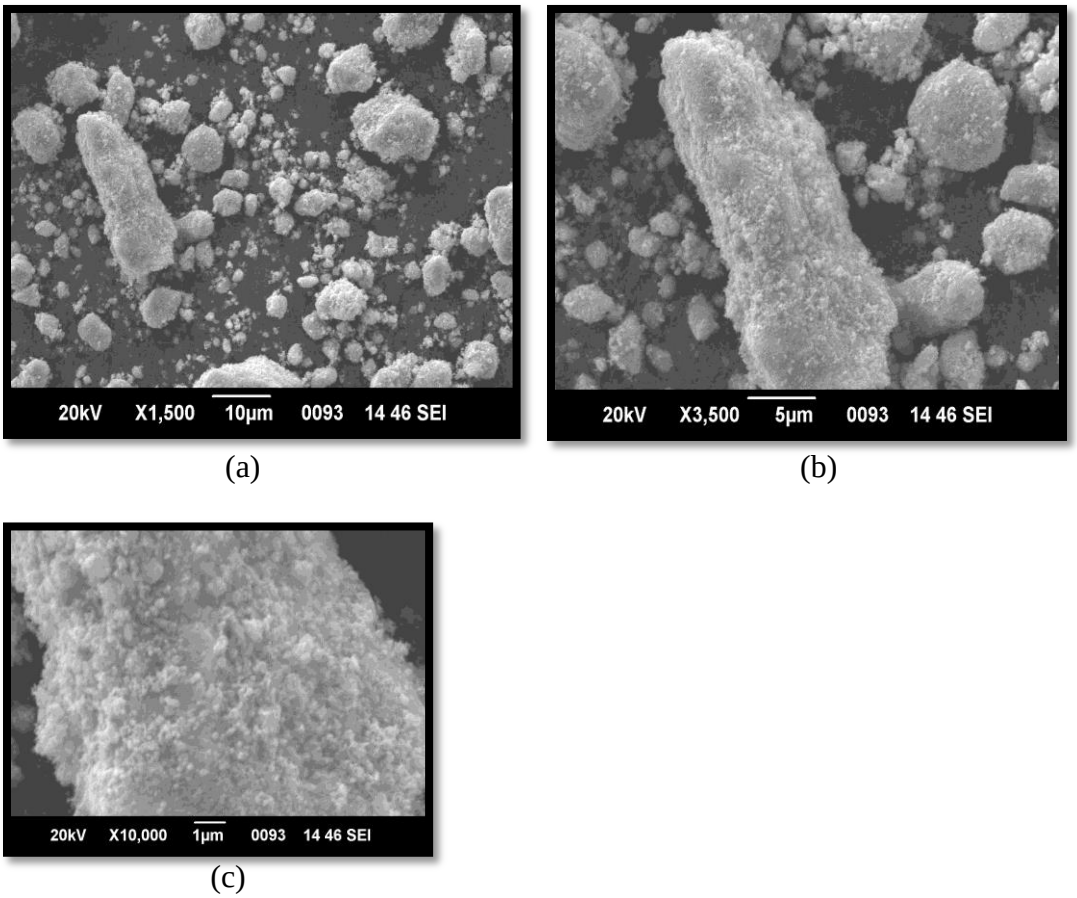

(a) (b)

(c)

*Fig 3.3 SEM images of pure SnO_2 nanopowder, magnification of (a)*10µm *(b)*5µm *(c)*1µm.

3.1.3 UV-VIS Spectrscopic Analysis

3.1.3 (a) Energy band gap from Tauc plot

The Absorption Spectrum of Pure SnO_2 nanopowder is shown below

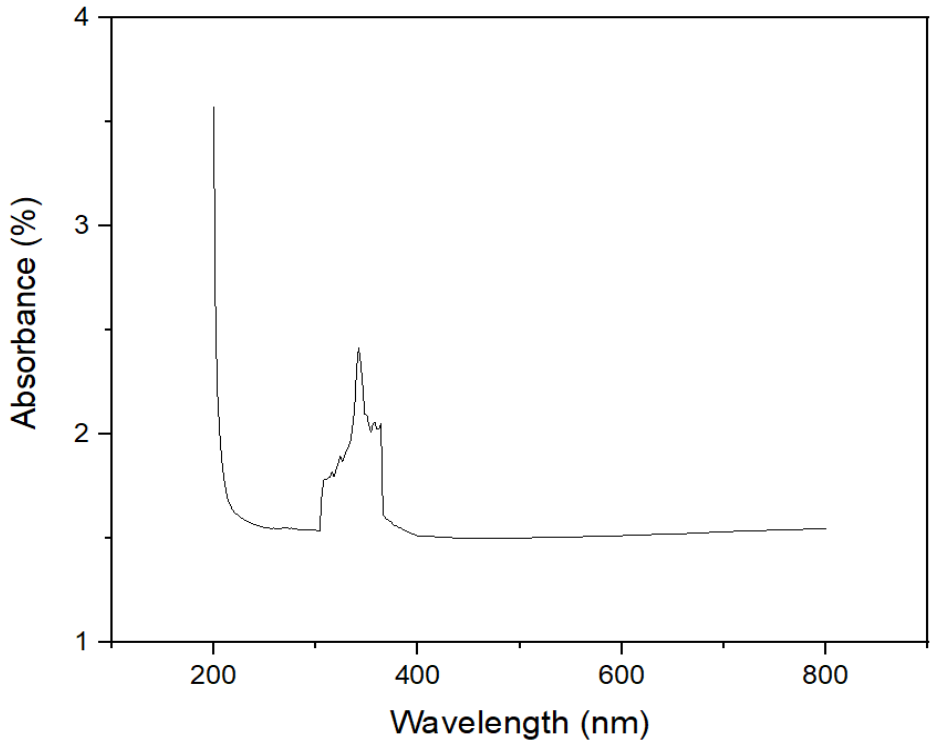

Fig 3.4 Absorption Spectrum of Pure SnO_2 Nanopowder

The bandgap energy of SnO_2 was determined using Tauc plot analysis, a method commonly employed to assess the optical properties of materials. This analysis involves correlating the absorption coefficient (α) with the incident photon energy (hν) using a relation that incorporates a constant (A) and a power factor (n), typically (1/2) for direct transitions. By plotting the square of the absorption coefficient multiplied by photon energy ((αhν)^2) against photon energy (hν), researchers can identify the bandgap energy. In the case of SnO_2nanopowder, the bandgap energy was extrapolated from the linear portion of the ((αhν)^2) curve to zero, yielding a value of **3.4eV**. This determination provides valuable insights into the material's electronic and optical characteristics, essential for various applications in optoelectronics and semiconductor devices.

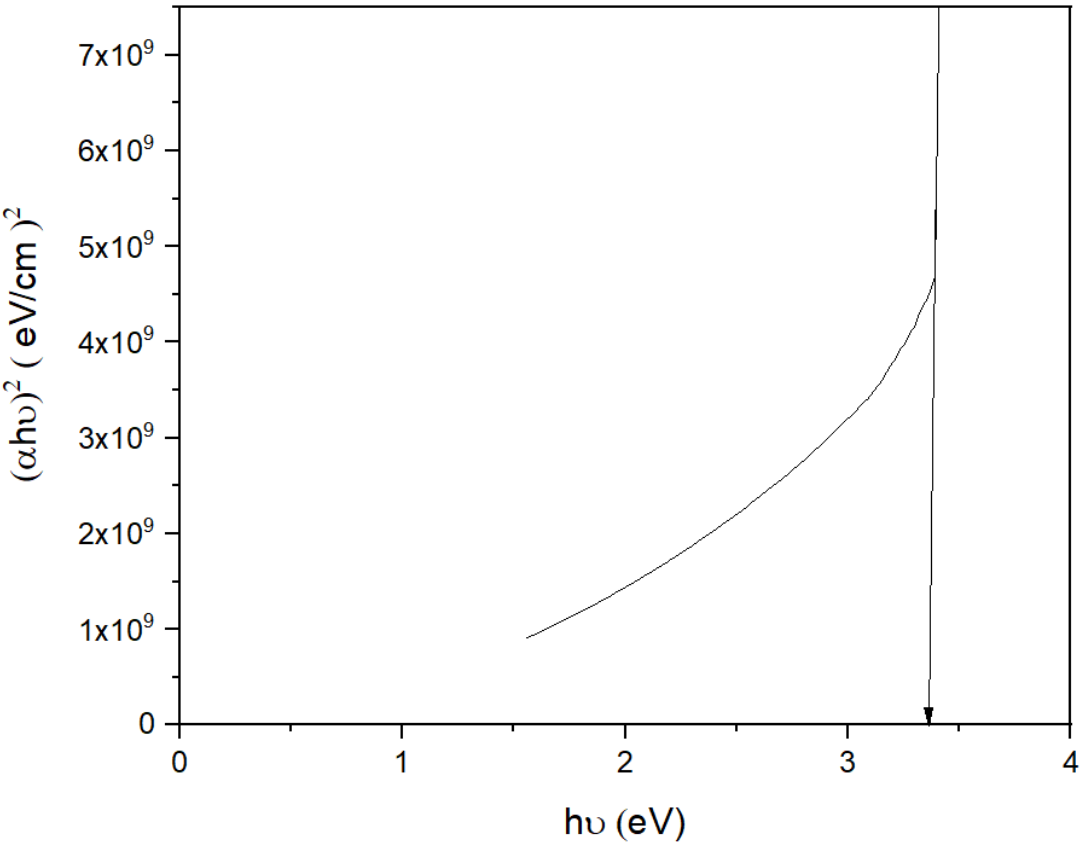

Fig 3.5 Tauc plot of Pure SnO_2 nanopowder

3.1.3 (b) Photocatalytic Degradation rate

The photocatalytic activity of pure tin oxide nanopowder solution in the presence and absence of light over methyl orange dye was observed after 24 and 48 hours. Over time, a color change from pale orange to a clear solution was noticed, indicating the degradation of methyl orange.

Figure.3.6 Methyl orange solution with SnO_2 NPs after 24 hour and after 48 hour placed under irradiation of direct sunlight

To evaluate the degradation rate, the samples were analyzed using UV-Visible spectroscopy. The figures below show the wavelength versus absorbance graphs of pure tin oxide nanopowder solution in the presence of light over methyl orange dye for the given time periods.

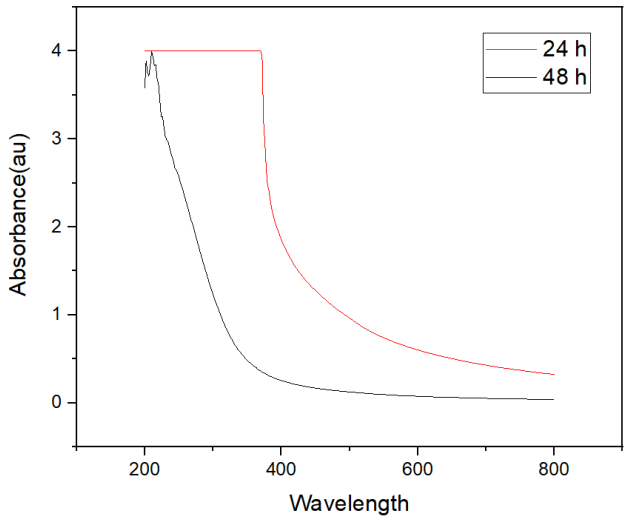

Figure.3.7 Photocatalytic degradation of methyl orange dye under the irradiation of direct light using SnO_2*NPs*

By extrapolating the wavelength versus absorbance curve to the absorbance axis (y-axis), the corresponding absorbance percentage can be determined. From the absorbance percentage, the degradation percentage can be calculated using the equation:

$$\text{Degradation percentage} = \left[\frac{AO - At}{AO}\right] \times 100$$

where Ao is the absorbance of the dye solution after 24 hours, and At is the absorbance of the dye solution after 48 hours.

At=0.387 Ao=1.439

$$\text{Degradation percentage} = \left[\frac{1.439-0.387}{1.439}\right] \times 100$$

$$= 73.1\%$$

Similarly, the photocatalytic activity of pure tin oxide nanopowder solution in the absence of light over methyl orange dye was observed after 24 and 48 hours, with a noticeable color change.

The figures below show the wavelength versus absorbance graphs of pure tin oxide nanopowder solution in the absence of light over methyl orange dye for the given time periods.

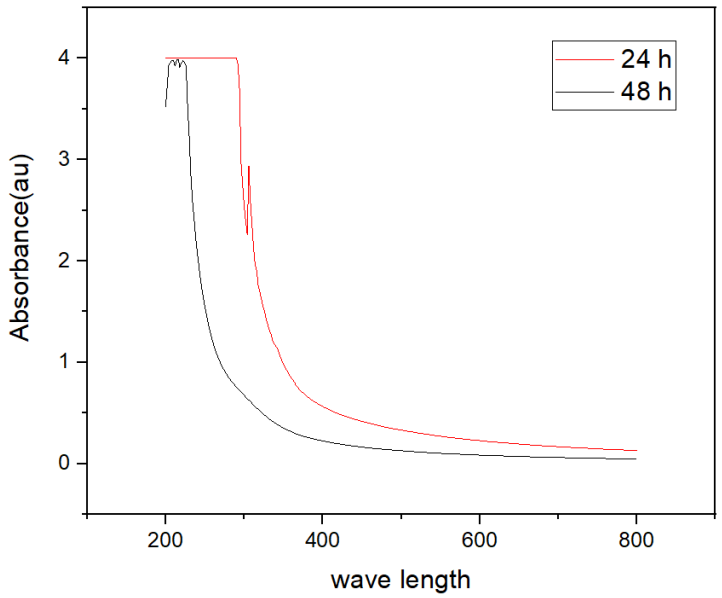

Figure.3.8 Photocatalytic degradation of methyl orange dye in absence of light using SnO_2*NPs*

The absorbance percentage was determined, and from this, the degradation percentage was calculated.

$$\text{Degradation percentage} = \left[\frac{AO - At}{AO}\right] \times 100$$

At=0.266 Ao=0.614

$$\text{Degradation percentage} = \left[\frac{0.614 - 0.266}{0.614}\right] \times 100$$

$$= 56.68\ \%$$

3.2 CADMIUM DOPED TIN-OXIDE NANOPOWDER

3.2.1 XRD Analysis

The structural characteristics of the specimens were scrutinized via X-ray diffraction (XRD) pattern examination. Numerous elements affect the development of the nanopowder, including precursor composition, reaction parameters, and reaction duration. XRD is a widely used technique for investigating material crystallography. For our investigation, we constructed a plot with 2θ along the X-axis and Intensity along the Y-axis using Origin software. The acquired data was juxtaposed with values from the JCPDS database for comparative analysis.

For cadmiumdoped tin oxide, the X-ray diffraction pattern revealed peaks at 2θ angles of 33.835,37.933,51.739 and 54.722 degrees, corresponding to the Miller indices (1 0 1), (2 0 0), (2 1 1), and (2 2 0), respectively. This indicates that the cadmium doped tin oxide exhibit tetragonal structures.

To determine the average grain size of the samples, we utilized the Debye-Scherrer formula:

$$\boldsymbol{D = \frac{0.9\,\lambda}{\beta\, cos\theta}}$$

This formula allows us to evaluate the grain size based on the XRD data obtained.

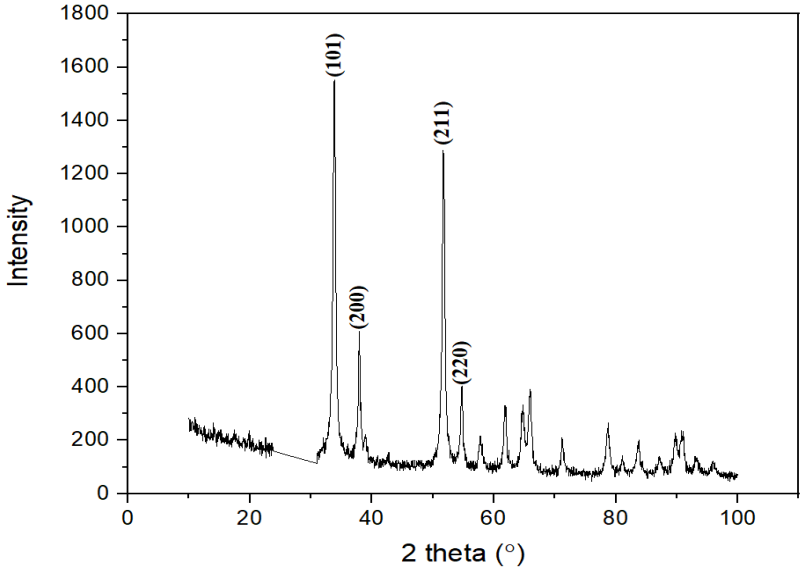

Fig 3.9 XRD Analysis graph of Cadmium doped tinoxide Nanopowder

3.2.1(a) Crystalline size

To derive the crystalline size and average crystalline size from XRD data, we must first pinpoint the peaks corresponding to the crystal planes of interest in the X-ray diffraction (XRD) pattern. These peaks offer insights into the material's structural attributes. Once identified, we measure the full width at half maximum (FWHM) of each peak, indicating its angular width at half of its maximum intensity. Additionally, we determine the peak position (θ) in radians.

With these parameters established, we apply the Scherrer equation:

$$\boldsymbol{D = \frac{0.9\,\lambda}{\beta\,cos\theta}}$$

Here, D represents the crystalline size (in nanometers), λ denotes the wavelength of the X-ray source (typically 0.15418 nm), β signifies the FWHM in radians, θ stands for the peak position in radians, and 0.9 serves as a commonly utilized constant factor.

By substituting the measured values of β and θ, alongside the known values of λ and 0.9, into the Scherrer equation, we can calculate the crystalline size for each peak. In case multiple peaks are analyzed, the average crystalline size can be computed by averaging the individual crystalline sizes obtained from each peak.

This methodology furnishes valuable insights into the structural attributes of materials, facilitating the characterization and comprehension of their crystalline composition.

Peak position (2 theta)	FWMH	Crystalline size D (nm)	D nm (Average)
19.957	1	8.066309329	**10.53850441**
26.564	0.913	8.940449531	
33.823	0.869	9.555082031	
37.909	0.869	9.665995611	
51.687	0.869	10.157773	
54.773	0.869	10.29578739	
57.816	0.913	9.939835207	
61.815	0.869	10.65489434	
64.727	0.695	13.53267412	
65.988	0.782	12.11232036	
71.16	0.869	11.24041636	
78.767	0.913	11.25775452	
83.765	0.956	11.16152164	
87.069	1	10.95824832	

Table 3.6 Crystalline size of Cd doped SnO_2 calculated using Debye Scherrer's Equation

The dislocation density defined as the length of dislocation lines per unit volume is calculated from the crystalline size D using the equation

$$\text{dislocation density } (\delta) = \frac{1}{D^2}$$

$$\delta = \frac{1}{10.538^2}$$

$$\delta = 0.009$$

3.2.1(b) Texture Coefficent

Texture coefficient analysis is a method used to understand the favored alignment of crystalline domains within nanoparticles. This technique involves calculating the texture coefficient, TC(hkl), for specific crystallographic planes. The formula for TC(hkl) is:

$$\boldsymbol{TC(hkl)} = \frac{\boldsymbol{I(hkl)}}{\frac{\mathbf{1}}{\boldsymbol{N}} \boldsymbol{\Sigma}\, \boldsymbol{I(hkl)}}$$

Where:

- $\boldsymbol{TC(hkl)}$ is the texture coefficient for the hkl plane.

- $\boldsymbol{I(hkl)}$ is the intensity of each plane.

- $\boldsymbol{N}$ is the number of reflections.

A high TC value indicates a strong preference for alignment along a particular crystallographic plane within the nanoparticles. This alignment can significantly influence the properties and applications of the nanoparticles.

h k l	TC(hkl)
1 0 1	1.743
2 0 0	0.491
2 1 1	1.425
2 2 0	0.34

Table 3.7 texture coefficent of each hkl plane

3.2.1 (c) d-Spacing or Interplanar Spacing

To determine the interplanar spacing (d spacing) from XRD data using Bragg's equation, we employ the formula:

$$\boldsymbol{d = \frac{n\,\lambda}{2\,d\,\sin\theta}}$$

Where:

- $\lambda = 1.5418$ Å (wavelength of incident X-ray)

- θ represents the peak position (in radians)

- $n = 1$ (order of diffraction)

- d is the interplanar spacing or d spacing (in Å)

Initially, we need to identify the peak position from the XRD data. Then, by substituting this value into the equation, we can calculate the interplanar spacing.

2 theta (deg)	theta (deg)	d-spacing (Å)
33.83497	16.917485	2.647132056
37.93275	18.966375	2.37005755
51.73915	25.869575	1.765431004
54.72238	27.36119	1.676028804

Table 3.8 d spacing of Cd doped SnO_2 calculated using bragg's equation.

3.2.1 (d) Grain size from WH Plot

The Williamson-Hall (W-H) method was employed to analyze the diffraction line broadening resulting from strain and reduced grain size. This method utilizes Equation (2),

$$\beta \cos\theta = 0.9\,\lambda/D + 2\xi \sin\theta \qquad (2)$$

where β represents the full width at half maximum of the diffraction peak, θ denotes the glancing angle, ξ signifies the lattice strain, and D is the average grain size calculated via Scherrer's formula. Equation (2) can be rewritten as Equation (3),

$$\beta \cos\theta = \xi\,(2\sin\theta) + 0.9\,\lambda/D \qquad (3)$$

which depicts a straight line with ξ as its gradient (slope) and (0.9 λ)/(D) as its y-intercept. By comparing Equation (3) to the standard equation of a straight line (Equation 4),

$$y = mx + c \qquad (4)$$

we establish the relationships:

$y = \beta \cos\theta$

$m = \xi$

$x = 2 \sin\theta$ and

$c = (0.9\,\lambda)/(D)$

Here, 'm' represents the slope, indicating the strain ξ, while the y-intercept (0.9 λ)/(D) is used to calculate the crystallite size. Subsequently, the plot of 2sinθ on the x-axis and βcosθ on the y-axis is presented below.

2theta (deg)	theta (rad)	FWMH (deg)	FWMH (rad)	2 sinθ	β Cosθ
33.83497	0.295266	0.60253	0.01051613	0.581988	0.010061

37.93275	0.331026	0.54526	0.00951658	0.650026	0.009
51.73915	0.451509	0.58399	0.01019255	0.872648	0.009171
54.72238	0.477543	0.45579	0.00795504	0.919197	0.007065

Table 3.9 values of βcosθ and 2sin θ for SnO_2*NPs.*

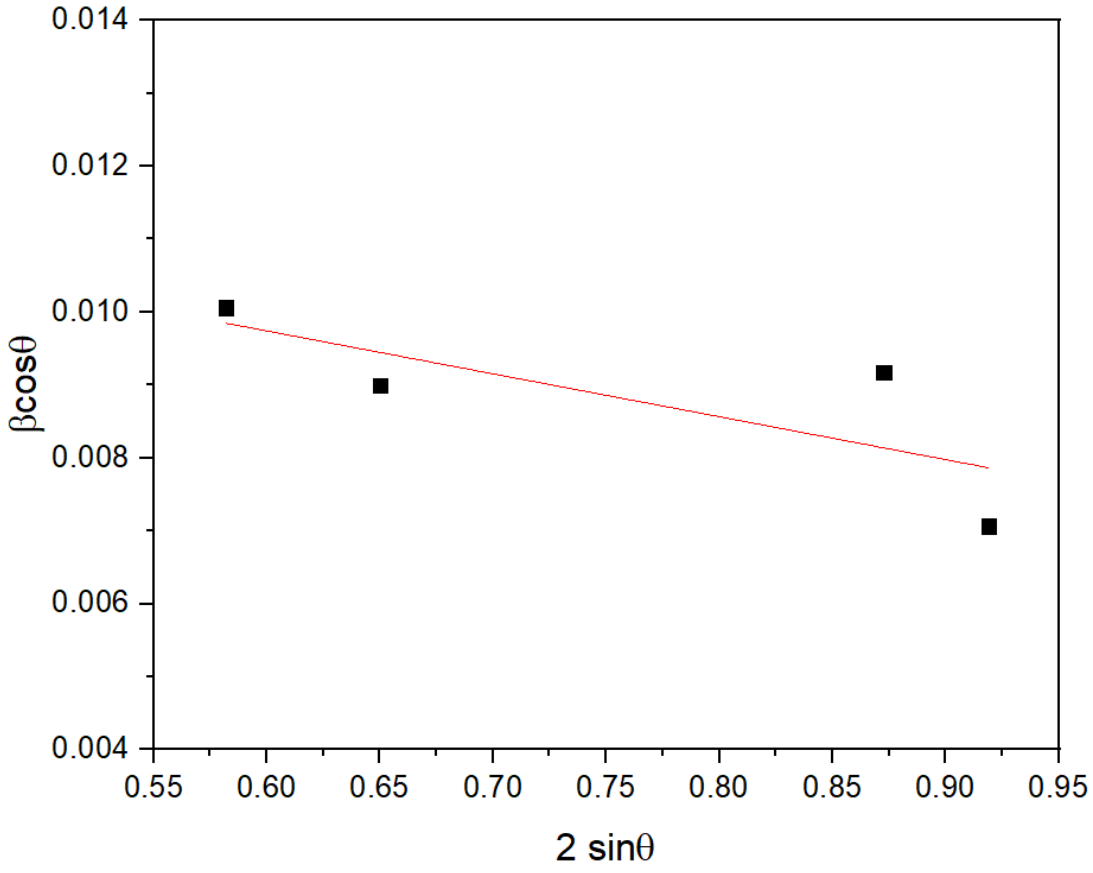

Fig 3.10 To calculate crystalline size and strain from XRD data using Williamson-Hall (W-H) plot method for Cd doped SnO_2*NPs.*

Slope of the plot is the strain.So the value of strain (ξ) = -0.00326
The value of y-intercept "c" = 0.01202

$$\text{y-intercept } \mathbf{c}=0.9\ \lambda/D$$

Or

$$D=0.9\ \lambda/c$$

Where the shape factor and λ = 0.15406 nm is the wavelength of the X-ray source,putting all these values we get,

$$D = \frac{0.9 \times 0.15406}{0.01327}$$

$$D = \frac{0.138654}{0.01327}$$

$$D = 10.449 \text{ nm}$$

COMPOUND	Grain size (D) from Scherrer's Formula (nm)	Grain size (D) from W-H plot (nm)
CADMIUM DOPED TIN OXIDE NANOPOWDER	**10.538**	**10.449**

Table 3.10 Grain size comparisson data of Cd doped SnO_2 from Debye Scherrer's Equation and W-H plot

The reduction of grain size in SnO_2 (tin oxide) nanopowder upon doping with Cd (cadmium) is primarily due to the introduction of lattice strain and distortion, caused by the difference in ionic

radii between Sn^{4+} and Cd^{2+}. This strain inhibits the growth of SnO_2 grains, leading to smaller sizes. Additionally, Cd doping increases the number of nucleation sites during synthesis, distributing the available material among more nuclei and resulting in smaller grains. Changes in surface energy due to Cd presence can also alter growth kinetics, further promoting finer grains. Moreover, Cd atoms at grain boundaries act as pinning forces, hindering grain boundary movement and growth. Lastly, the altered thermodynamic stability of Cd-doped SnO_2 compared to pure SnO_2 affects grain growth dynamics, contributing to the reduced grain size.

3.2.2 Scanning Electron Microscope (SEM)

SEM images captured at magnifications of 10µm, 5µm, and 1µm reveal agglomerated SnO_2nanoparticles synthesized via the Precipitation method. Although the exact size of individual particles cannot be determined from these images, TEM analysis offers this capability. The micrograph suggests that the particles exhibit irregular shapes, prompting further analysis using a particle analyzer to ascertain their sizes accurately.

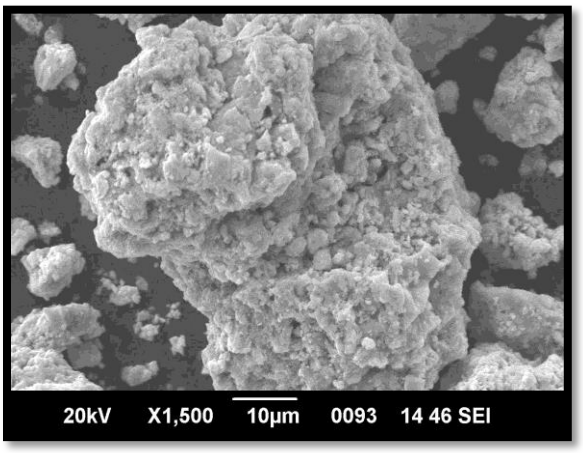

(a)

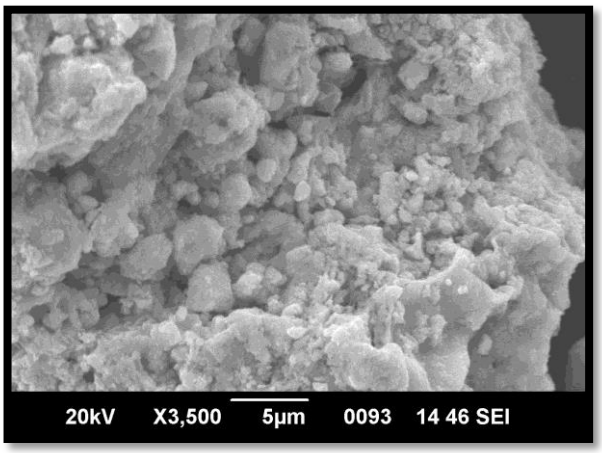

(b)

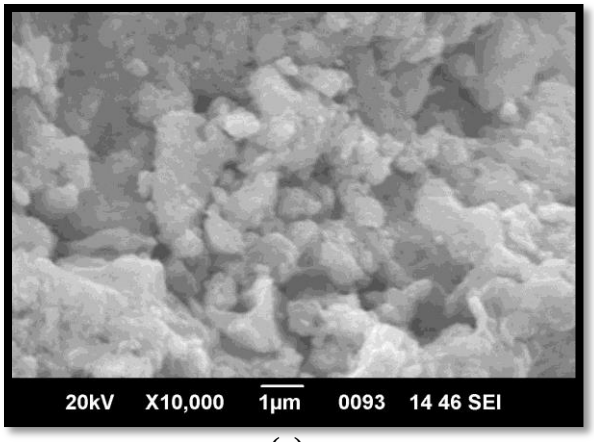

(c)

*Fig 3.11 SEM images of Cd doped SnO_2 nanopowder, magnification of (a)*10µm *(b)*5µm *(c)*1µm.

3.2.3 UV-VIS Spectrscopic Analysis

The Absorption Spectrum of Cd doped SnO_2 nanopowder is shown below

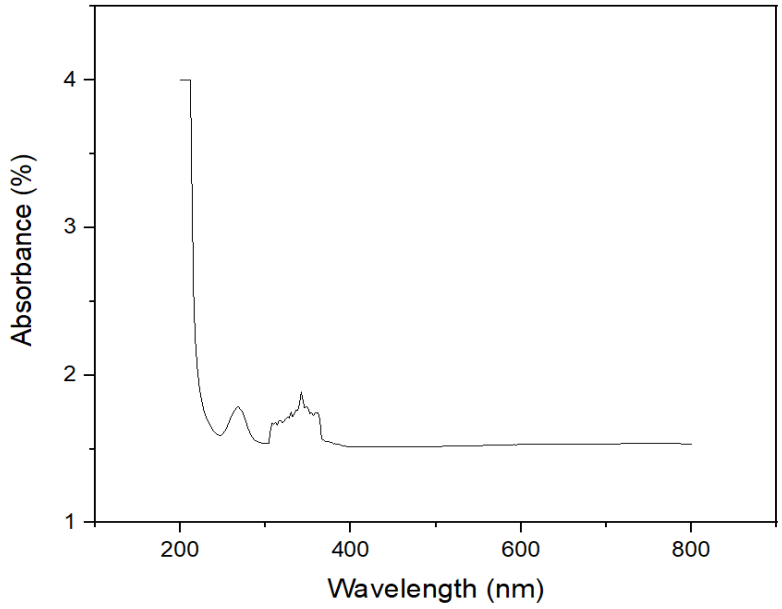

Fig 3.12 Absorption Spectrum of Cd dooped SnO_2 Nanopowder

The bandgap energy of $SnO_2$was determined using Tauc plot analysis, a widely used method for evaluating the optical properties of materials. This technique involves correlating the absorption

coefficient (α) with the incident photon energy (hν) using a relation incorporating a constant (A) and a power factor (n), typically (1/2) for direct transitions. By plotting the square of the absorption coefficient multiplied by photon energy ((αhν)^2) against photon energy (hν), researchers can pinpoint the bandgap energy. For SnO_2thin films, the bandgap energy was extrapolated from the linear section of the ((αhν)^2) curve to zero, resulting in a value of **3.3 eV**. This determination offers crucial insights into the material's electronic and optical properties, crucial for various applications in optoelectronics and semiconductor devices.

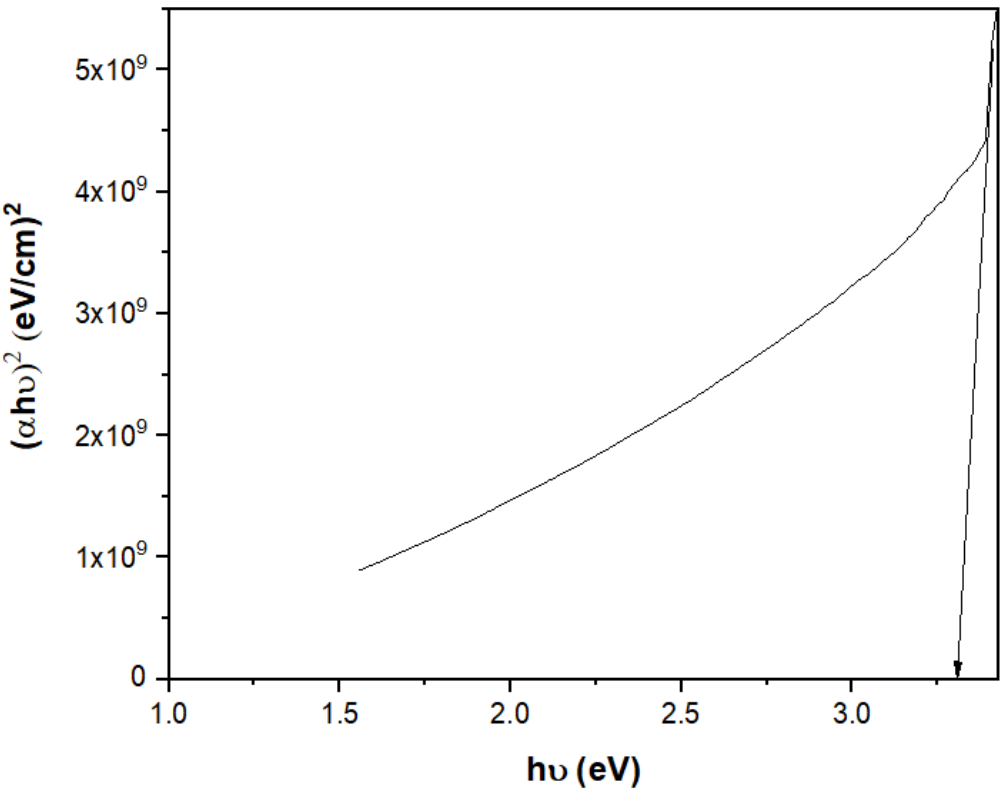

Fig 3.13 Tauc plot of Cd doped SnO_2 nanopowder

The decrease in the band gap of SnO_2 (tin oxide) nanopowder upon doping with Cd (cadmium) can be attributed to several factors. Firstly, Cd doping introduces impurity states within the band gap, which act as intermediate energy levels and narrow the gap by facilitating electron transitions. Additionally, the incorporation of Cd causes lattice distortion and strain due to the difference in ionic radii between Cd^{2+} and Sn^{4+}, modifying the electronic band structure. Increased charge carrier concentration from Cd doping leads to band tailing, where the edges of the

conduction and valence bands become less defined, effectively reducing the band gap. Furthermore, the hybridization of Cd orbitals with those of Sn and O alters the energy levels of the bands, contributing to the band gap reduction. Lastly, quantum confinement effects in nanopowders are modified by Cd doping, further decreasing the band gap.

CHAPTER 4

CONCLUSION AND FUTURE SCOPE

4.1 Conclusion

Pure SnO_2 and Cd-doped SnO_2nanopowder were successfully prepared using the precipitation method. The resultant samples were analyzed using various techniques such as XRD, UV-Vis spectroscopy, and SEM.

The XRD results showed a reduction in crystalline size upon doping, as determined by Scherrer's formula: 12.6 nm for pure $SnO_2$and 10.54 nm for Cd-doped SnO_2samples. From the Williamson-Hall (WH) plot, the grain size was calculated to be 10.748 nm for SnO_2 and 10.449 nm for Cd-doped SnO_2nanoparticles, indicating a tetragonal structure. The orientation of crystalline domains within the nanoparticles was analyzed by determining the texture coefficient of hkl planes, and the interplanar distance was obtained using Bragg's equation.

UV-Visible spectroscopy analysis revealed that the band gap energy decreased by 0.1 eV upon doping. The photocatalytic activity analysis of pure SnO_2in a methyl orange solution showed a degradation percentage of 73.1% in the presence of light and 56.68% in the absence of light, indicating that light is a significant factor in enhancing the degradation rate.

SEM images at magnifications of 10µm, 5µm, and 1µm revealed the granular structures of both compounds.

4.2 Future scope

The future scope of SnO_2 (tin oxide) nano powder is quite promising due to its unique properties and wide range of potential applications. In gas sensing, SnO_2 nano powder's high sensitivity to various gases makes it an excellent material for sensors, with future developments likely to focus on enhancing sensitivity, selectivity, and stability for detecting gases like CO, NO_2, and H_2. In photocatalysis, its wide band gap and high stability make SnO_2 a good candidate for applications such as water splitting for hydrogen production and organic pollutant degradation in wastewater. Research is ongoing to improve its efficiency under visible light and to develop composite materials with enhanced properties. Transparent conducting films, which use SnO_2 in touchscreens, displays, and photovoltaic cells, may see improvements in conductivity and transparency, as well as the development of flexible and more efficient electronic devices. SnO_2 nano powder also shows promise as an anode material in lithium-ion batteries, with future research addressing issues like volume expansion during charge-discharge cycles to enhance battery performance and longevity. In solar cells, particularly as an electron transport layer in perovskite solar cells, advancements may aim at improving efficiency, stability, and scalability for commercial use. Additionally, SnO_2 nanoparticles have antimicrobial properties, which can be

optimized for use in coatings, textiles, and medical devices. Environmental remediation is another promising area, with SnO_2 nanoparticles used to remove pollutants from air and water due to their high surface area and reactivity. Finally, SnO_2 is utilized as a catalyst in various chemical reactions, such as CO oxidation and hydrocarbon combustion, with future research likely to enhance its catalytic efficiency, durability, and selectivity. Overall, the future scope of SnO_2 nano powder is broad and multidisciplinary, with significant potential for impacting various technological and industrial fields.

REFERENCES

1. Introduction to nanotechnology Charles P Poole Jr. and Frank J Owens ,John Wiley & Sons, 2003

2. Nanomaterials and Nanocomposites - Synthesis, Properties, Characterization Techniques, and Applications, Rajendra Kumar Goyal, CRC Press

3. Faculty of Science and Technology, Technological and Higher Education Institute of Hong Kong Correspondence to: Chi-Wing Tsang, Changhai Liang

4. Synthesis of SnO_2 nanoparticles through the controlled precipitation route
C. Ararat Ibarguen

5. Kumar, R., et al. (2018). Tin oxide nanoparticles: synthesis, characterization and application in environmental pollution control. Journal of Materials Science, 53(13), 8721-8746.

6. Synthesis and characterization of ZnO nano-particles, Jayanta Kumar Behera- Department of physics NIT Rourkela

7. A study on MgO NPs synthesis,Capping and antibacterial property, Muhammed Ashiq ul islam- Department of physics Farook College, Calicut